Experimental and Analytical Investigations of the Dynamic Response of Adhesively Bonded Single Lap Joints

A. Vaziri

H. Nayeb-Hashemi

Department of Mechanical,
Industrial and Manufacturing Engineering,
Northeastern University,
Boston, MA 02115

H. R. Hamidzadeh
Department of Mechanical Engineering,
Tennessee State University,
Nashville, TN 37221

Dynamic response of single lap joints, subjected to a harmonic peeling load is studied theoretically and experimentally. In the theoretical part, dynamic response of a single lap joint clamped at one end and subjected to a harmonic peeling load at the other end is investigated. Adherents are modeled as Euler-Bernouli beams joined in the lap area by a viscoelastic adhesive layer. Both axial and transverse deformations of adherents are considered in deriving the equations of motion. The effects of adhesive layer thickness, mechanical properties and its loss factor on the dynamic response of the joint are investigated. Furthermore, effects of defects such as a void in the lap area on the dynamic response of the joints are studied. The results showed that frequencies where peak amplitudes occurred were little dependent on the adhesive loss factor. However, peak amplitudes reduced for joints with a higher adhesive loss factor. Furthermore, the results indicated that for the joint geometries and properties investigated the system resonant frequencies were not affected by the presence of a central void covering up to 80% of the overlap length. In the experimental part, single lap joints were fabricated using 6061-T6 Aluminum. Adherents were joined together using Hysol EA 9689 adhesive film. Joints with various central voids were manufactured by removing adhesive film from the desired area of lap joints prior to bonding adherents. Dynamic responses of the joints were investigated using the hammer test technique. The system response was measured using both an accelerometer and a noncontact laser vibrometer. The natural frequencies of the joints obtained by using the laser vibrometer were very close to those obtained theoretically. However, natural frequencies obtained by using an accelerometer depended on the accelerometer location in the system, which was attributed to its mass contribution to the overall system mass. A central void covering less than 80% of the overlap length had little effect on the system resonance frequencies. This was in agreement with the theoretical results. In contrast total system-damping ratios were a function of the void size. Joints without a void exhibited higher damping. [DOI: 10.1115/1.1596550]

Introduction

Joining components by using adhesives is an attractive method compared to other joining techniques and is becoming more popular with the development of adhesives with high adhesion properties. The ease of manufacturing, surface appearances, stress distribution in the bond area, cost of manufacturing and capabilities of joining dissimilar materials are some of the advantages of using adhesives. Despite of many advantages, their applications often proceed with caution. The bond strength and adhesive mechanical properties could be severely affected by improper surface preparations, curing procedure and entrapped void and porosity in the bond area. Confidence in using adhesives in joining components could be increased by understanding the effects of adhesive and adherents mechanical properties, adhesive thickness, voids, and porosities in the lap area, on the static and dynamic response of the joints. There are a number of papers reporting the stress distribution in single lap joints subjected to in-plane and out of plane static and dynamic loadings. A comprehensive literature survey on this subject has been presented in [1]. However, most of these studies have ignored the presence of defects in the lap area and their effects on the static and dynamic response of the lap joint and the shear and peel stress distributions in the bond area. Over the past five years we have studied effects of defects such as voids and disbond, adhesive properties, bonded joint geometries and properties on the strength of single lap joints subjected to axial and peeling loads, tubular joint strength under tension/torsion loading, thermal stress in the bonded joints and nondestructive evaluation of bonded joints [2–12].

There are a number of papers on the effects of large displacement on the stress distribution in adhesively bonded joints considering the adhesive layer as elastic, viscoelastic, and viscoplastic material [13–15]. These analyses have resulted in identification of critical zones for joint failure. Goto et al. [16] studied the frequency response of the five thermoplastic composites bonded by two kinds of epoxy resin. It was shown that vibration-damping properties increased by using flexible epoxy resin as adhesives. He and Rao [17] and [18] developed an analytical model to study vibration of bonded joints subjected to transverse loadings by considering both longitudinal and transverse displacements of the system. The equations of motion were developed using Hamiltonian principle. They obtained the system resonance frequencies, mode shapes and modal loss factors. However, there was no attempt to investigate the effects of the adherents and adhesive mechanical properties as well as defects in the lap area on the dynamic response of lap joints. Yuceoglu et al. [19] studied free bending vibrations of two rectangular orthotropic plates connected together by an adhesive layer in a single overlap configuration. The natural frequencies and corresponding mode shapes are obtained using Mindlin plate theory. It was found when the plate adherents were dissimilar, the upper plate experienced very different deflec-

Contributed by the Technical Committee on Vibration and Sound for publication in the JOURNAL OF VIBRATION AND ACOUSTICS. Manuscript received July 2001; Revised January 2003 Associate Editor A. F. Vakakis.

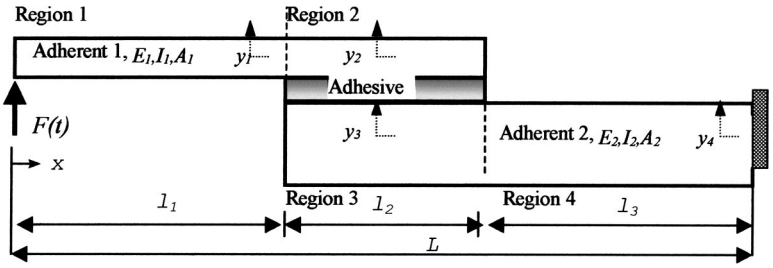

Fig. 1 Schematic Model for a single lap joint

tion shapes than those of the lower plate at least in the lower modes. In fact, one of the plates remained almost stationary, while the other, exhibited a dominant deflection shape.

Olia and Rossettos [12] derived the stress distribution in adhesively bonded joints with a gap subjected to bending. The results showed steep edge gradients for the peel and shear stresses and the peek stresses always occurred at the extreme end of the overlap. It was found that a void had little effect on the peak stresses, unless it was sufficiently close to the edge of the overlap.

The effects of bond geometry and adhesive properties on vibration response of single lap joints under harmonic peeling load were studied by Vaziri et al. [20]. Furthermore, the effects of a void in the lap joint, on the natural frequencies and damping behavior of the joint and peeling and shear stresses amplitude distribution were studied [2,3,20]. The results showed that for the type of adherents and adhesive analyzed, a void up to 60 percent of the overlap length had a negligible effect on the vibration response and peel and shear stresses distribution. However, these analyses ignored the axial deformation of adherents and its coupling with bending deformation in formulating the dynamic response of the lap joint. The objective of this paper is (1) to study the dynamic response of single lap joints subjected to a harmonic peeling load by considering the axial deformation of adherents, (2) to understand the effects of defects such as a void in the overlap on the system response and (3) to verify our theoretical results by experimental investigations.

Theoretical Investigation

Schematic diagram of a single lap joint subjected to a harmonic peeling load, $F(t)$, is shown in Fig. 1. The stress distribution in the bonded area is obtained by modeling the adherents as Euler Bernoulli beams supported on a viscoelastic foundation which resist both peeling and shear deformations. The axial and transverse equations of motion are obtained by dividing the beam into four regions and writing the equilibrium equations for each region. The peel stress is assumed to be proportional to $k(y_i-y_j)$, where k is the stiffness of the elastic foundation and is assumed to be $k=(E_a w/h_0)$, E_a is the elastic modulus of adhesive layer, w is the width of the overlap, h_0 is the adhesive thickness and y_i and y_j are transverse displacements of upper and lower adherents in a particular location respectively.

Considering the axial and transverse displacements of adherents, the shear stress in the bonded area can be expresses as,

$$\tau=\frac{G}{2h_0}\left[2u_2-2u_3+h_1\frac{\partial y_2}{\partial x}+h_2\frac{\partial y_3}{\partial x}\right] \tag{1}$$

Where G is the adhesive shear modulus, h_1 and h_2 are the thickness of adherents and y_2, y_3, and u_2 and u_3 are the axial and transverse displacements of adherents right at the top and bottom of the adhesive layer. The adhesive is considered to be viscoelastic and its shear modulus is assumed to be $G=G_0(1+i\eta)$, where η is the adhesive loss factor and G_0 is the real part of the adhesive shear modulus.

Considering the free body diagram of an element in the region two, Fig. 2, the equilibrium equations are:

$$\frac{\partial V}{\partial x}+\ddot{y}_2(\rho A)_1+k(y_2-y_3)=0 \tag{2}$$

$$V-\frac{\partial M}{\partial x}+\tau w\frac{h_1}{2}=0 \tag{3}$$

$$\frac{\partial}{\partial x}\left(E_1A_1\frac{\partial u_2}{\partial x}\right)-\tau w=\frac{\partial^2}{\partial t^2}(\rho A)_1u_2 \tag{4}$$

Similarly, the equation of motion for the third region can be presented as:

$$\frac{\partial V}{\partial x}+(\rho A)_2\ddot{y}_3+k(y_3-y_2)=0 \tag{5}$$

$$V-\frac{\partial M}{\partial x}+\tau w\frac{h_2}{2}=0 \tag{6}$$

$$\frac{\partial}{\partial x}\left(E_2A_2\frac{\partial u_3}{\partial x}\right)+\tau w=\frac{\partial^2}{\partial t^2}(\rho A)_2u_3 \tag{7}$$

Considering the relation between transverse displacement and bending moment from the beam theory:

$$M=(EI)\frac{\partial^2 y}{\partial x^2} \tag{8}$$

Eqs. (2), (3), and (8) can be simplified to:

$$(\rho A)_1\ddot{y}_2+k(y_2-y_3)+(EI)_1\frac{\partial^4 y_2}{\partial x^4}-w\frac{h_1}{2}\frac{\partial \tau}{\partial x}=0 \tag{9}$$

Similarly, Eqs. (5), (6), and (8) yields:

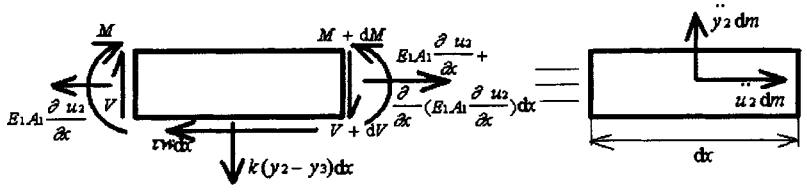

Fig. 2 Free body diagram for an element in region 2

$$(\rho A)_2\ddot{y}_3+k(y_3-y_2)+(EI)_2\frac{\partial^4 y_3}{\partial x^4}-w\frac{h_2}{2}\frac{\partial \tau}{\partial x}=0 \quad (10)$$

The equilibrium equations for regions 1 and 4 are those of classical Euler Bernouli beam equations. Substituting Eq. (1) into Eqs. (9) and (10), the governing equations of motion for each regions of the bonded joint can be presented as,

$$(EI)_1\frac{\partial^4 y_1}{\partial x^4}+(\rho A)_1\ddot{y}_1=0 \quad (11)$$

$$(EA)_1\frac{\partial^2 u_1}{\partial x^2}-(\rho A)_1\frac{\partial^2 u_1}{\partial t^2}=0 \quad (12)$$

$$(EI)_1\frac{\partial^4 y_2}{\partial x^4}+(\rho A)_1\ddot{y}_2+k(y_2-y_3)-\frac{wh_1G}{4h_0}\left(2\frac{\partial u_2}{\partial x}-2\frac{\partial u_3}{\partial x}+h_1\frac{\partial^2 y_2}{\partial x^2}+h_2\frac{\partial^2 y_3}{\partial x^2}\right)=0 \quad (13)$$

$$(EI)_2\frac{\partial^4 y_3}{\partial x^4}+(\rho A)_2\ddot{y}_3+k(y_3-y_2)-\frac{wh_2G}{4h_0}\left(2\frac{\partial u_2}{\partial x}-2\frac{\partial u_3}{\partial x}+h_1\frac{\partial^2 y_2}{\partial x^2}+h_2\frac{\partial^2 y_3}{\partial x^2}\right)=0 \quad (14)$$

$$(EA)_1\frac{\partial^2 u_2}{\partial x^2}-\frac{wG}{h_0}\left(u_2-u_3+\frac{h_1}{2}\frac{\partial y_2}{\partial x}+\frac{h_2}{2}\frac{\partial y_3}{\partial x}\right)-(\rho A)_1\frac{\partial^2 u_2}{\partial t^2}=0 \quad (15)$$

$$(EA)_2\frac{\partial^2 u_3}{\partial x^2}+\frac{wG}{h_0}\left(u_2-u_3+\frac{h_1}{2}\frac{\partial y_2}{\partial x}+\frac{h_2}{2}\frac{\partial y_3}{\partial x}\right)-(\rho A)_2\frac{\partial^2 u_3}{\partial t^2}=0 \quad (16)$$

$$(EA)_2\frac{\partial^2 u_4}{\partial x^2}-(\rho A)_2\frac{\partial^2 u_4}{\partial t^2}=0 \quad (17)$$

$$(EI)_2\frac{\partial^4 y_4}{\partial x^4}+(\rho A)_2\ddot{y}_4=0 \quad (18)$$

For a system subjected to a harmonic peeling force of $Fe^{i\omega t}$ at the system's free end, the displacement field for each region is:

$$y_j(x,t)=y_j(x)e^{i\omega t} \quad \text{where } j=1,2,3, \text{ and } 4. \quad (19)$$

$$u_j(x,t)=u_j(x)e^{i\omega t} \quad \text{where } j=1,2,3 \text{ and } 4. \quad (20)$$

Equations (11) to (18) can be presented in nondimensionalized forms by considering the following nondimensionalized parameters,

$$\beta_j=\frac{G_o}{E_j} \quad \text{where } j=1 \text{ and } 2. \quad (21)$$

$$a_1=\frac{(\rho A)_1\omega^2L^4}{(EI)_1} \quad (22)$$

$$a_2=\frac{kL^4}{(EI)_1} \quad (23)$$

$$a_3=\beta_1\frac{wh_1^2L^2}{4h_0I_1}(1+i\eta) \quad (24)$$

$$a_4=\frac{(\rho A)_2\omega^2L^4}{(EI)_2} \quad (25)$$

$$a_5=\beta_1\frac{wh_1h_2L^2}{4h_0I_1}(1+i\eta) \quad (26)$$

$$a_6=\beta_2\frac{wh_1h_2L^2}{4h_0I_2}(1+i\eta) \quad (27)$$

$$a_7=\beta_2\frac{wh_2^2L^2}{4h_0I_2}(1+i\eta) \quad (28)$$

$$a_8=\frac{kL^4}{(EI)_2} \quad (29)$$

$$a_9=\beta_1\frac{wL^2}{h_0A_1}(1+i\eta) \quad (30)$$

$$a_{10}=\beta_1\frac{wh_2L^2}{h_0A_1h_1}(1+i\eta) \quad (31)$$

$$a_{11}=\beta_2\frac{wL^2}{h_0A_2}(1+i\eta) \quad (32)$$

$$a_{12}=\frac{\rho_1\omega^2L^2}{E_1} \quad (33)$$

$$a_{13}=\beta_2\frac{wh_2L^2}{h_0A_2h_1}(1+i\eta) \quad (34)$$

$$a_{14}=\frac{\rho_2\omega^2L^2}{E_2} \quad (35)$$

$$\overline{y_i}=y_i/h_1 \quad (36)$$

$$\overline{u_i}=u_i/(h_1^2/2L) \quad (37)$$

$$\zeta=\frac{x}{L}, \quad \text{and} \quad \zeta_1=\frac{l_1}{L}, \quad \text{and} \quad \zeta_2=\frac{l_1+l_2}{L} \quad (38)$$

$$\text{where } L=l_1+l_2+l_3 \quad (39)$$

Incorporating the above nondimensional parameters into equations of motions results in,

$$\frac{\partial^4\overline{y_1}}{\partial\zeta^4}-a_1\overline{y_1}=0 \quad (40)$$

$$\frac{\partial^2\overline{u_1}}{\partial\zeta^2}+a_{12}\overline{u_1}=0 \quad (41)$$

$$\frac{\partial^4\overline{y_2}}{\partial\zeta^4}-a_1\overline{y_2}+a_2(\overline{y_2}-\overline{y_3})-a_3\frac{\partial^2\overline{y_2}}{\partial\zeta^2}-a_5\frac{\partial^2\overline{y_3}}{\partial\zeta^2}-a_3\frac{\partial\overline{u_2}}{\partial\zeta}+a_3\frac{\partial\overline{u_3}}{\partial\zeta}=0 \quad (42)$$

$$\frac{\partial^4\overline{y_3}}{\partial\zeta^4}-a_4\overline{y_3}+a_8(\overline{y_3}-\overline{y_2})-a_6\frac{\partial^2\overline{y_2}}{\partial\zeta^2}-a_7\frac{\partial^2\overline{y_3}}{\partial\zeta^2}-a_6\frac{\partial\overline{u_2}}{\partial\zeta}+a_6\frac{\partial\overline{u_3}}{\partial\zeta}=0 \quad (43)$$

$$\frac{\partial^2\overline{u_2}}{\partial\zeta^2}-a_9\left(\overline{u_2}-\overline{u_3}+\frac{\partial\overline{y_2}}{\partial\zeta}\right)-a_{10}\frac{\partial\overline{y_3}}{\partial\zeta}+a_{12}\overline{u_2}=0 \quad (44)$$

$$\frac{\partial^2\overline{u_3}}{\partial\zeta^2}+a_{11}\left(\overline{u_2}-\overline{u_3}+\frac{\partial\overline{y_2}}{\partial\zeta}\right)+a_{13}\frac{\partial\overline{y_3}}{\partial\zeta}+a_{14}\overline{u_3}=0 \quad (45)$$

$$\frac{\partial^2\overline{u_4}}{\partial\zeta^2}+a_{14}\overline{u_4}=0 \quad (46)$$

$$\frac{\partial^4\overline{y_4}}{\partial\zeta^4}-a_4\overline{y_4}=0 \quad (47)$$

The solution to Eq. (40) is in the form of:

$$\overline{y_1}=\sum_{j=1}^{4}A_{1j}e^{S_{1j}\zeta}, \quad \text{where } S_{11}=\sqrt[4]{a_1}, \quad S_{12}=-\sqrt[4]{a_1},$$

$$S_{13}=i\sqrt[4]{a_1}, \quad \text{and} \quad S_{14}=-i\sqrt[4]{a_1} \tag{48}$$

Similarly, solutions to Eqs. (41 and 46–47) are,

$$\overline{y_4}=\sum_{j=1}^{4} A_{4j}e^{S_{4j}\zeta}, \quad \text{where} \quad S_{41}=\sqrt[4]{a_4}, \quad S_{42}=-\sqrt[4]{a_4},$$

$$S_{43}=i\sqrt[4]{a_4}, \quad \text{and} \quad S_{44}=-\sqrt[4]{a_4} \tag{49}$$

$$\overline{u_1}=\sum_{j=1}^{2} A_{3j}e^{S_{3j}\zeta}, \quad \text{where} \quad S_{31}=i\sqrt{a_{12}} \quad \text{and} \quad S_{32}=-i\sqrt{a_{12}} \tag{50}$$

$$\overline{u_4}=\sum_{j=1}^{2} A_{5j}e^{S_{5j}\zeta}, \quad \text{where} \quad S_{51}=i\sqrt{a_{14}} \quad \text{and} \quad S_{52}=-i\sqrt{a_{14}} \tag{51}$$

The solutions for the displacement fields corresponding to that of Eqs. (42–45) are in the form of,

$$\overline{y_2}=\sum_{j=1}^{12} A_{2j}e^{S_j\zeta}, \tag{52}$$

$$\overline{y_3}=\sum_{j=1}^{12} t_{1j}A_{2j}e^{S_j\zeta}, \tag{53}$$

$$\overline{u_2}=\sum_{j=1}^{12} t_{2j}A_{2j}e^{S_j\zeta}, \tag{54}$$

and

$$\overline{u_3}=\sum_{j=1}^{12} t_{3j}A_{2j}e^{S_j\zeta} \tag{55}$$

where S_j's are roots of the characteristic equations and t_{ij} ($i=1$ to 3 and $j=1$ to 8) can be calculated from the governing equations of displacement. Details of displacement field calculations are provided in [20]. Similar equations are also developed for bonded joints containing a void in the overlap area by dividing the overlap to three regions [20]. Here we will present the results without stating the corresponding equations.

Experimental Investigation

Adhesively bonded joints were prepared by using 6061-T6 aluminum bars with thickness of 3.17 and 12.6 mm, and width of 25.4 mm as adherents. Aluminum bars were joined together in a single lap configuration using Hysol EA 9689 epoxy film of 0.13 mm thickness. The adherents' surfaces in the bond area were sand blasted and cleaned with acetone prior to bonding. The overlap area was 25.4 mm×25.4 mm. Shims of 0.08 mm was used during manufacturing of joints in order to maintain adhesive thickness among various specimens. Voids of various sizes were introduced in the lap area by cutting the adhesive film and removing it from the bond area prior to manufacturing joints. Mold release agent was sprayed in the void area to ensure no adhesion from any possible adhesive seepage to the void area. The lap joints dimensions corresponding to Fig. 1 were $l_1=113.9$ mm, $l_2=25.4$ mm, and $l_3=113.9$ mm.

Dynamic responses of the bonded joints were obtained by clamping the free end of the thicker adherent to a rigid wall and striking the system with a wood hammer. Both contact and non-contact methods were used to record the dynamic responses of the joints. In the contact method, the effects of accelerometer location on the system response was studied by systematically changing its location and evaluating the joint response. In the non-contact method Laser Dropper Vibrometer were used to record the dynamic responses of bonded joints at its free end. A typical dynamic response and its corresponding frequency spectrum for a joint struck by wood hammer and using an accelerometer and a Laser Doppler to record its responses are shown in Figs. 3, 5 and 4, 6, respectively.

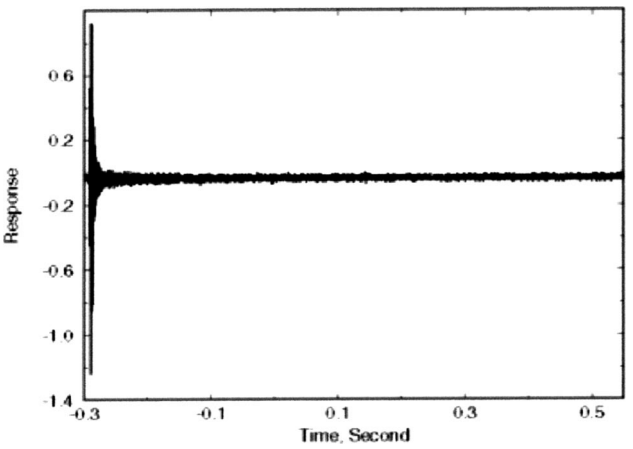

Fig. 3 A typical dynamic response of a bonded joint struck by a wood block hammer, using an accelerometer to record the system response

Resonant frequencies were identified from the peaks in the frequency spectrum, Figs. 4 and 6, and the system damping ratios were obtained from the quality factor Q. Although the hammer test excites many resonant frequencies, the response frequencies corresponding to those of the theoretical investigation where identified. Their shift with the adhesive geometry and properties were recorded. A typical procedure for evaluating damping ratios corresponding to the frequency spectrum is shown in Fig. 7. The damping ratio was obtained by evaluating ω_1 and ω_2 corresponding to half power, Fig. 7. A MATLAB program was developed to find the best fit to the frequency spectrum from which maximum amplitude and half power points were identified.

The damping ratio was obtained from,

$$Q\approx\frac{1}{2\zeta}\approx\frac{\omega_n}{\omega_2-\omega_1} \tag{56}$$

The results indicate that the accelerometer location has a significant effect on the system response. Changing the accelerometer location from the free end to a location close to the clamped end resulted in 35% reduction in the system first resonant frequency. This was related to the contribution of accelerometer's mass to the

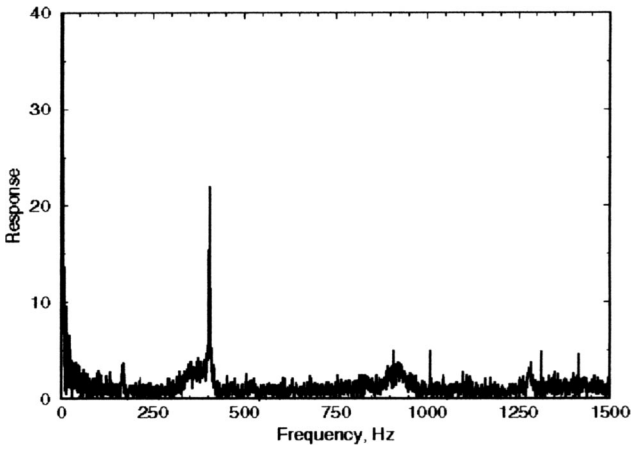

Fig. 4 Frequency spectrum corresponding to the system response shown in Fig. 3, used to identify resonant frequencies obtained theoretically

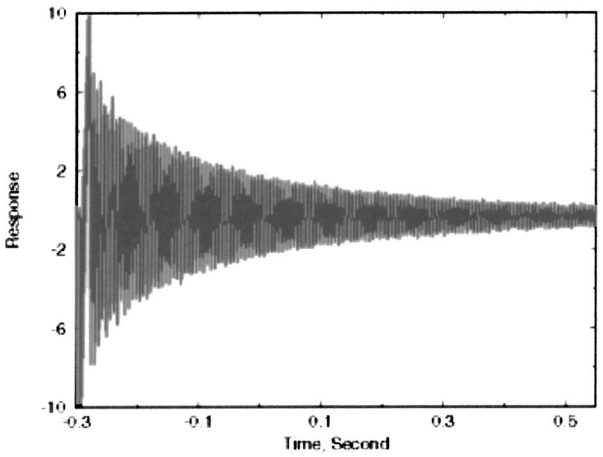

Fig. 5 A typical dynamic response of a bonded joint struck by a wood block hammer, using a noncontact laser vibrometer

total mass of the system. For this reason contact tests were performed with the accelerometer attached at a distance of 25.4 mm from the clamped end. For this experimental set-up, the accelerometer contribution, in reducing the system resonant frequencies was less than 2%. The result further showed that the hammer strike point did not have a significant effect on the measured resonant frequencies and damping ratio of the structure. The data presented in this paper were obtained from hammer tests by striking the system at its free end.

Table 1 Mechanical properties of the adhesive and adherents

E (Adherents)	G_0 (Adhesive)	ρ (Adherents)	ρ (Adhesive)
69 GPa	0.8 GPa	2710 kg/mm^2	1200 kg/mm^2

Results and Discussions

MATLAB based codes were written to analyze displacements and relating shear and peeling stresses. The results were obtained for similar joints as those used in the experimental investigations. The mechanical properties of the adhesive and adherents used in the theoretical investigations are listed in Table 1. Since there was no data on the adhesive loss factor, the adhesive loss factor was taken as a variable and its effect on the system response was investigated. No attempt was made to measure the actual adhesive loss factor, however, the total system damping ratio was obtained experimentally.

Figures 8 and 9 show the transverse and axial frequency responses of the joints at the location of the applied force for joints with different adhesive loss factors. The results indicate that the

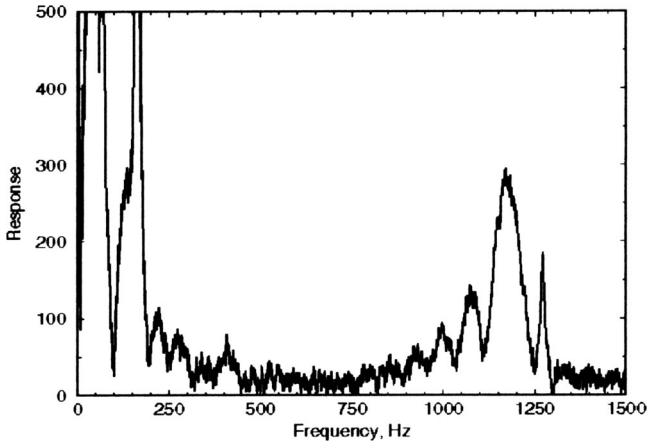

Fig. 6 Frequency spectrum corresponding to the system response shown in Fig. 5, used to identify resonant frequencies obtained theoretically

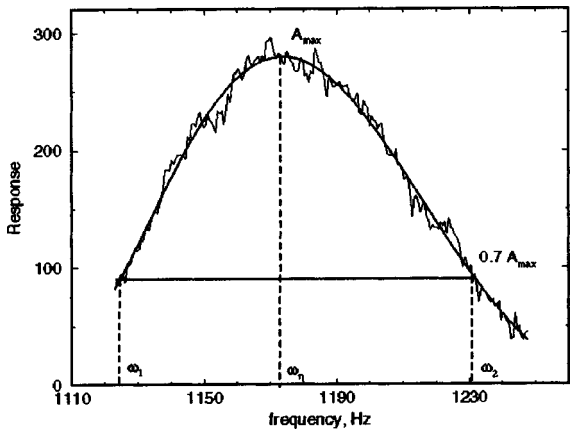

Fig. 7 A portion of a frequency response used to identify and to measure natural frequency and damping ratio ζ

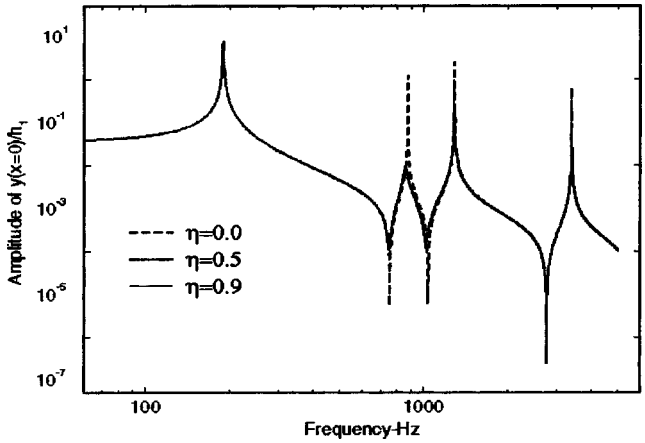

Fig. 8 Transverse frequency response at the free end of the adhesively bonded joints with various adhesive loss factors. Joints were subjected to 1 N harmonic peeling load.

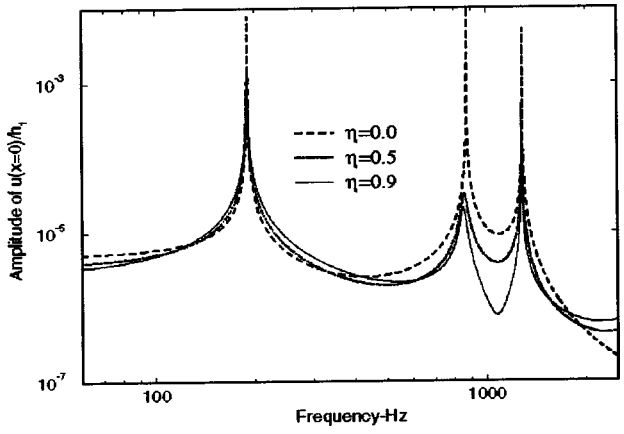

Fig. 9 Axial frequency response at the free end of the adhesively bonded joints with various adhesive loss factors. Joints were subjected to 1 N harmonic peeling load.

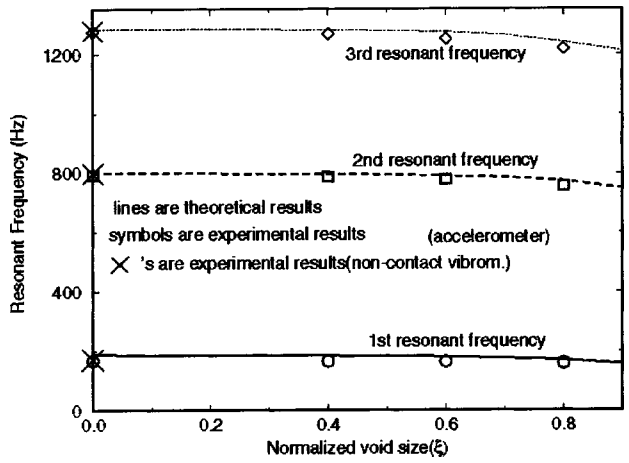

Fig. 10 Effect of the void size on the first three resonant frequencies of bonded joints

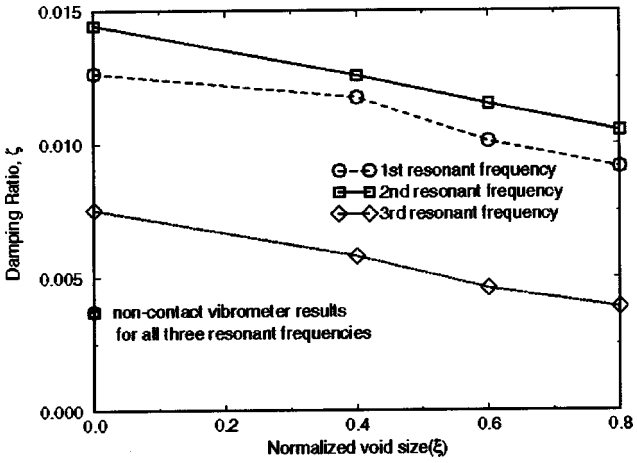

Fig. 11 Damping ratio of bonded joints vs. central void size

first two resonant frequencies are close to those of adherent 1 with a fixed end. The third and fourth are also close to the resonant frequencies of the second adherent. These results could be justified considering the lap joint geometries. The first adherent is relatively thinner than the second adherent. Therefore first and second mode shapes could be considered to be that of adherent one with a fixed end. The fixed end in this case is the bonded area. The results indicate that for these frequencies there were little displacements in the second adherent. The results further indicate that considering axial deformation of adherents in deriving the equations of motion resulted in only 2% increase in the resonance frequencies when compared to the results presented in [2–3]. This is due to the fact that bending stiffness of the system dominates the dynamic response of the system. Furthermore, Figs. 8 and 9 indicate that adhesive damping has a significant effect on the transverse amplitude where peak amplitudes occur and has a negligible effect when the frequency of applied load is far from the system resonant frequencies. In contrast, the effect of adhesive damping on the axial amplitude is more pronounced over a large range of applied loading frequencies.

Figure 10 shows the theoretical and experimental results of the effect of a central void size on the first three resonant frequencies of the system. Experimental results were obtained using an accelerometer attached to the system close to the fixed end for all tests and a non-contact Laser Doppler Vibrometer for specimens with no defects. The results indicate that the measured natural frequencies using these two methods are within 2% of each other and the accelerometer mass at the installed position has a negligible effect on the system resonant frequencies. Each experimental data point is the mean value of at least three experiments for each specimen. Furthermore, the experimental data are within 8% of the theoretical values for joints with and without a void. This could be due to error in the experimental setup such as a slight variation in the clamping position, resulting in some variation in the over all system length, contribution of the accelerometer mass to the overall system mass, which was not considered in the theoretical investigation and the changes in the adhesive mechanical properties due to variation in the curing time. Results indicate that for the joints investigated a void size covering up to 80% of the overlap length has little effect on the resonant frequencies of the structure. It was also observed that a void location apparently has greater effect on resonant frequencies than the void size. A similar conclusion was reached in [2–3].

The modal damping ratios of joints with and without a void were also evaluated. Figure 11 shows the effect of void size on the modal damping ratios. Results show that damping ratios decreases with increasing the void size. This is consistent with the loss of adhesive from the joint area and its energy dissipation capacity. Damping ratios of joints without a void was also obtained, using a noncontact vibrometer. The damping ratio seems to be much smaller when the noncontact vibrometer was used to measure the system response. The exact reason for this discrepancy between two methods is not know at this time. However, this could be due to the limited experiments performed using the non-contact method and the contribution of accelerometer to the over all system response and its damping. A new laser droppler vibrometer is currently being acquired and we will further investigate the effect of using an accelerometer vs. non-contact method on measured vibrational parameters.

Figures 12–14 show the effects of the joint dimensional parameters on the first resonant frequency. Results indicate that the system first resonant frequency initially increases drastically with the overlap length, Fig. 12. However, further increase in the overlap length may have little effect on the system first resonant frequency. The overlap length apparently has greater effect when $h_2/h_1=1$. This could be justified considering that both adherents contributing equally to the system stiffness. In addition, it was observed that the first natural frequency asymptotically approaches to the natural frequency of adherent 1 for $h_2/h_1>2$. However, the magnitude of the natural frequency depends on the ratio of elastic modulus of adhesive to adherent. These results could be justified considering the bending rigidity of adherent 2. Increasing adherent 2 thickness makes it to behave as a rigid element, thus it contributes little to the system natural frequency. Adherent 1, thus can be assumed to be supported by an elastic

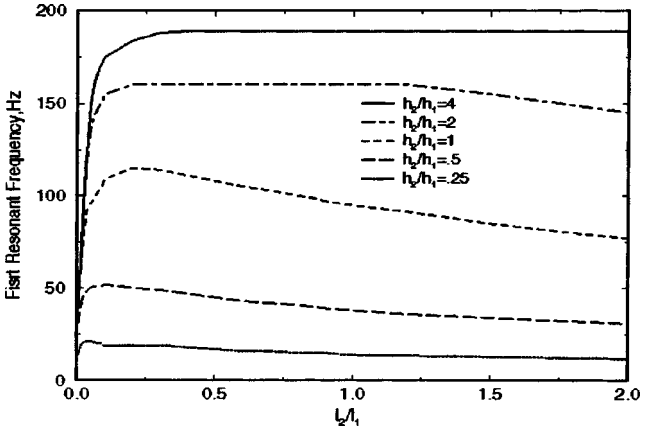

Fig. 12 First resonant frequency of the bonded joint vs. overlap length l_2/l_1, for joints with various h_2/h_1

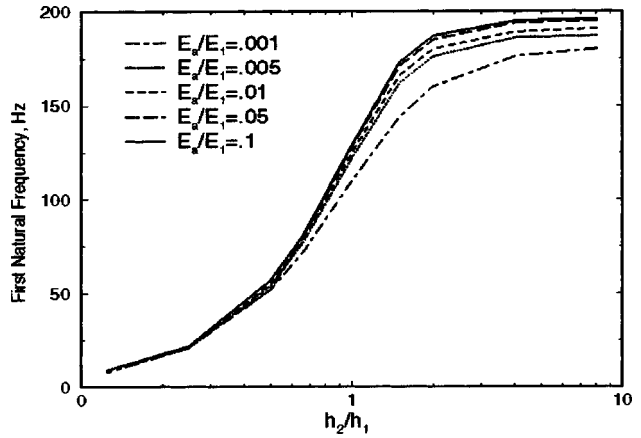

Fig. 13 Variation of the first resonance frequency vs. h_2/h_1 for several E_a/E_1

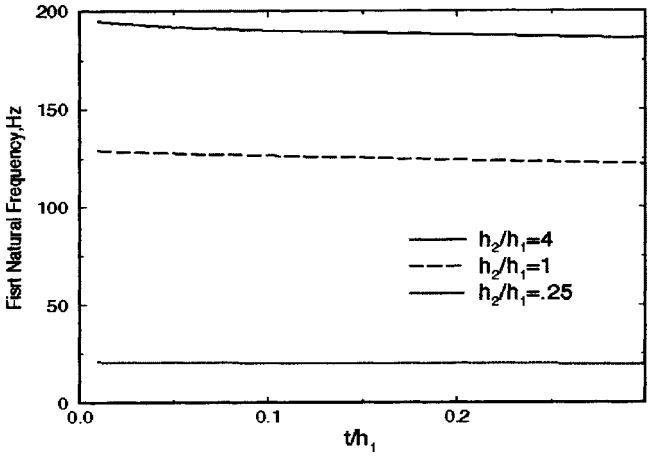

Fig. 14 Variation of the first resonance frequency vs. adhesive thickness, t/h_1, for several h_2/h_1 ratios

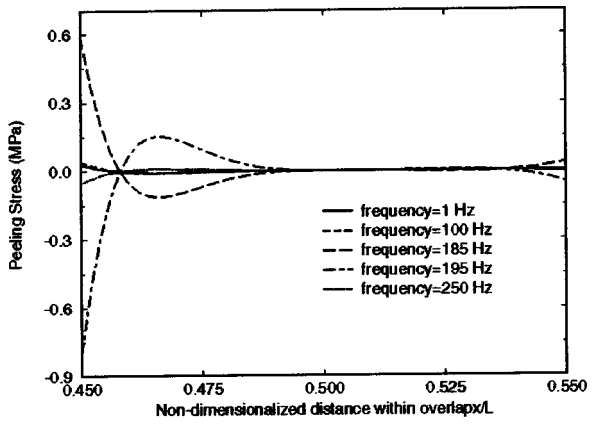

Fig. 15 Distribution of peeling stress amplitude within the overlap for the bonded joint subjected to a 1 N harmonic force at five different frequencies. Adhesive was assumed to be elastic with $\eta=0$.

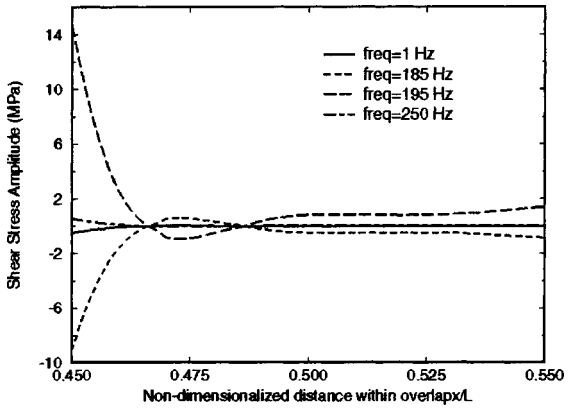

Fig. 16 Distribution of shear stress amplitude within the overlap for the bonded joint subjected to a 1 N harmonic force at five different frequencies. Adhesive was assumed to be elastic with $\eta=0$.

foundation on a rigid element. Furthermore, For bonded joint with $h_2/h_1<1$, the natural frequency seems to be little affected with the adhesive properties, Fig. 13. The results also do not show any asymptotic value for the natural frequency with h_2/h_1 ratio. These results again can be justified considering that the system response is mainly controlled with low bending rigidity of the adherent 2 and both adhesive and adherent 1 have little effect on the system natural frequency. The effect of adhesive thickness on the system natural frequency is shown in Fig. 14. The results indicate that for the range of adhesive thickness studied in this part, the system natural frequency decreases with increasing adhesive thickness. This can be explained considering the system stiffness is reduced with increasing the adhesive thickness.

The distribution of the peeling and shearing stresses along the overlap for a joint with no adhesive damping are shown in Figs. 15 and 16 for several harmonic loading frequencies. The peel and shear stresses are significantly higher as the frequency of the applied load approaches the first natural frequency. It is observed that considering the axial deformation in deriving the equations of motion does not significantly affect the magnitude and distribution of peeling stress. In contrast, the shear stress amplitude distribution significantly differs from those in [3], when considering the adherent axial deformation in deriving the equations of motion.

Conclusions

Dynamic response of the adhesively bonded joints with and without a defect in the lap area was obtained by modeling the lap joints as Euler-Bernouli beams supported on an elastic foundation, which resist both peeling and shear stresses. Both axial and transverse displacements were considered in deriving the coupled equations of motion. The system resonant frequencies and the peel and shear stress distributions were obtained for several forcing frequencies.

Based on the analyses, it was found that the first natural frequencies of the system correspond to the natural frequency of adherents. The experimental results indeed confirmed the theoretical results for resonant frequencies. The resonant frequencies of the system were little sensitive to the damping value of the adhesive. Depending on the adherents thickness, the resonant frequencies of the system asymptotically approached to one of adherents resonant frequencies, clamped at one end.

The results indicate that for the joint geometries and mechanical properties investigated the resonant frequencies are little affected with the presence of a central void size, covering 80% of the over lap length. The resonant frequencies initially increase drastically with increasing the overlap length. However, further increase in the overlap length does not change the resonant fre-

quencies significantly. The peel and shear stresses in the overlap were obtained. The maximum shear and peel stresses were confined to the edges of the overlap.

Resonant frequencies and modal damping ratio were obtained for joints with and without a void experimentally, using both an accelerometer to record the system response and a noncontact Laser Doppler method. The results indeed confirmed those results obtained from the theoretical investigations that the system resonant frequencies are little affected with a central void size covering up to 80% of the overlap length. In contrast, the system modal damping ratios decrease with increasing the void size.

The maximum peel and shear stress in the lap area are confined to the edge of the overlap, and their magnitude increases as the frequency of the applied load approaches the natural frequency of the system. The direction of peeling and shear stress changes as the frequency of the applied load sweeps over the first natural frequency and becomes out of phase respect to the applied load.

Nomenclature

A_i = cross sectional area of the ith adherent
E_i = modulus of elasticity of the ith adherent
E_a = modulus of elasticity of the adhesive
$F(t)$ = applied force
G_o = real part of shear modulus of the adhesive
G = complex shear modulus of the adhesive
h_i = thickness of the ith adherent
I_i = moment of inertia of the ith adherent
k = stiffness per unit length of the adhesive
l_i = length of the ith section
L = overall length of the bonded joint
h_o = adhesive thickness
w = width of the beams
y_i = transverse displacement of the ith section
u_i = axial displacement of the ith section
η = adhesive loss factor
ρ_i = density of the ith adherent
τ = shear stress
ω = peeling load frequency

References

[1] Tsai, M. Y., and Morton, J., 1994, ''Evaluation of Analytical and Numerical Solutions to the Single-lap Joint,'' Int. J. Solids Struct., **31**(18), pp. 2537–2563.

[2] Vaziri, A., Hamidzadeh, H. R., and Nayeb-Hashemi, H., 2001, ''Dynamic Response of Bond Strength With Void Subjected to a Harmonic Peeling Load,'' J. Multibody Dynamics (Proc. Instn. Mech. Engrs., Part K), **215**(4), pp. 199–206.

[3] Vaziri, A., Hamidzadeh, H. R., and Nayeb-Hashemi, H., 2001, ''Evaluation of the Bond Strength With a Void Subjected to a Harmonic Peeling Load,'' *Proceeding to the ASME Congress and Exposition: Vibration and Control*, November 10–15, New York, NY.

[4] Vaziri, A., and Nayeb-Hahsemi, H., 2002, ''Dynamic Response of the Tubular Joint with an Annular Void Subjected to a Harmonic Torsional Loading,'' J. Multibody Dynamics, **216**(4), pp. 361–371.

[5] Vaziri, A., and Nayeb-Hahsemi, H., 2002, ''Dynamic Response of the Tubular Joint with an Annular Void Subjected to a Harmonic Axial Loading,'' Int. J. Adhesion and Adhesives, **22**, pp. 367–373.

[6] Nayeb-Hashemi, H., Rossettos, J. N., and Melo, A. P., 1997, ''Multiaxial Fatigue Life Evaluation of Tubular Adhesively Bonded Joints,'' Int. J. Adhesion Adhesives, **17**, pp. 55–63.

[7] Rossettos, J. N., Lin, P., and Nayeb-Hashemi, H., 1994, ''Comparison of the Effects of Debonds and Voids in Adhesive Joints,'' ASME J. Eng. Mater. Technol., **116**, pp. 533–538.

[8] Nayeb-Hashemi, H., and Rossettos, J. N., 1994, ''Nondestructive Evaluation of Bonded Joints,'' Int. J. Acoustic Emission, **12**, pp. 1–14.

[9] Nayeb-Hashemi, H., and Jawad, O. C., 1997, ''Theoretical and experimental evaluation of the bond strength under peeling loads,'' ASME J. Eng. Mater. Technol., **119**(4), pp. 415–421.

[10] Nayeb-Hashemi, H., and Rosettos, J. N., 1994, ''Nondestructive Evaluation of Adhesively Bonded Joints,'' *Proceed. Symp. Cyclic Deformation, Fracture and Nondestructive Evaluation of Advanced Materials*, ASTM STP 1184, pp. 335–362.

[11] Rossettos, J. N., Peng, Y., and Nayeb-Hashemi, H., 1991, ''Analysis of Adhesively Bonded Composite Joints With Voids and Thermal Mismatch,'' *Proceedings to the Plastics and Plastic Composites: Material Properties, Part Performance, and Process Simulation*, ASME Winter Annual Meeting, Dec., Edited by V. J. Stokes, pp. 259–268.

[12] Olia, M., and Rossettos, J. N., 1996, ''Analysis of Adhesively Bonded Joints with Gaps Subjected to Bending,'' Int. J. Solids Struct., **33**, pp. 2681–2693.

[13] Pandey, P. C., Shankaragouda, H., and Singh, A. K., 1999, ''Nonlinear Analysis of Adhesively Bonded Lap Joints Considering Viscoplasticity in Adhesive,'' Comput. Struct., **70**(4), pp. 387–413.

[14] Apalak, M. K., and Engin, A., 1997, ''Geometrically Non-linear Analysis of Adhesively Bonded Double Containment Cantilever Joints,'' J. Adhesion Science and Technology, **11**(9), pp. 1153–1195.

[15] Austin, E. M., and Inman, D. J., 2000, ''Some Pitfalls of Simplified Modeling for Viscoelastic Sandwich Beams,'' ASME J. Vibr. Acoust., **122**, pp. 434–439.

[16] Got, A., Matsude, M., Hamade, H., Maekawa, Y., Maekawa, Z., and Matuo, T., 1993, ''Vibration Damping and Mechanical Properties of Continuous Fiber-Reinforced Various Thermoplastic Composites,'' *Int. SAMPE Symp. Exh., Proc. Adv. Mat.*, May 10–13, Vol. **38**(2), Anaheim CA, pp. 1651–1665.

[17] He, S., and Rao, M. D., 1992, ''Vibration Analysis of Adhesively Bonded Lap Joint. Part I: Theory,'' J. Sound Vib., **152**(3), pp. 405–416.

[18] Rao, M. D., and He, S., 1992, ''Vibration Analysis of Adhesively Bonded Lap Joint. Part II: Numerical Solution,'' J. Sound Vib., **152**(3), pp. 417–425.

[19] Yuceoglu, U., Toghi, F., and Tekinalp, O., 1996, ''Free Bending Vibration of Adhesively Bonded Orthotropic Plates With a Single Lap Joint,'' ASME J. Vibr. Acoust., **118**(1), Jan. New York NY, pp. 122–134.

[20] Vaziri, A., 2003, ''Dynamic Response of Bonded Joints with Defects,'' Ph.D. Thesis, Part I, Dept. of Mechanical Eng., Northeastern University, Boston, MA 02115.